

## Coherently walking, rocking and blinding single neutral atoms

This article has been downloaded from IOPscience. Please scroll down to see the full text article.

2011 J. Phys.: Conf. Ser. 264 012021

(<http://iopscience.iop.org/1742-6596/264/1/012021>)

View [the table of contents for this issue](#), or go to the [journal homepage](#) for more

Download details:

IP Address: 88.153.44.203

The article was downloaded on 31/07/2011 at 11:02

Please note that [terms and conditions apply](#).

# Coherently Walking, Rocking and Blinding Single Neutral Atoms

Artur Widera, Wolfgang Alt, and Dieter Meschede

Institut für Angewandte Physik, Universität Bonn, Wegelerstr. 8, 53115 Bonn, Germany

E-mail: [widera@uni-bonn.de](mailto:widera@uni-bonn.de)

**Abstract.** Advances in the preparation and detection, but most importantly in the coherent manipulation of single neutral atoms have allowed the observation of intriguing phenomena of quantum physics in recent years. We discuss developments to prepare and detect single neutral atoms in a one-dimensional optical lattice potential with single site resolution. Moreover, using two different experimental techniques, a state-dependent optical lattice potential on the one hand and a high-finesse optical cavity on the other hand, we have obtained coherent control over single neutral atoms. The former has enabled us to observe the quantum walk of atoms in position space, and to coherently control the motion of trapped atoms via microwave radiation. The latter offers a means to non-destructively detect the atomic spin state, thereby revealing quantum jumps of single atoms, or the altered optical properties of single atoms when subject to electromagnetically-induced transparency.

## 1. Introduction

Single neutral atoms have been, for a long time, envisioned to be candidates for a controlled assembly of interesting quantum states. Coherent control of internal and external atomic degrees of freedom lies at the heart of proposed quantum engineering procedures such as entanglement generation, quantum cellular automata, or single photon optical switching. Here we report on the implementation of two different tools for coherent control, a state dependent optical lattice and a high finesse optical resonator. Each system realises a text book example of quantum physics but at the same time yields novel insight into the feasibility and challenges for quantum state engineering with neutral atoms.

### *1.1. Preparation and Detection of Atoms with Single Site Resolution in an Optical Lattice*

We capture and cool single and few neutral caesium (Cs) atoms in a high-gradient magneto-optical trap and subsequently transfer the atoms into a far detuned, standing wave optical dipole trap (1D optical lattice) at  $\lambda = 866$  nm, see Fig. 1(a). By means of optical pumping we prepare the atoms in the  $|F = 4, m_F = +4\rangle$  state, where  $F$  is the total angular momentum and  $m_F$  its projection onto the quantisation axis along the lattice axis. This state is coherently coupled to  $|F = 3, m_F = +3\rangle$  by microwave radiation around 9.2 GHz, with which we obtain bare Rabi frequencies of up to  $\Omega_0/2\pi = 60$  kHz. State selective detection is performed by first applying a resonant laser pulse which removes selectively atoms in  $F = 4$ . Then, standard fluorescence imaging is used to image the configuration of the remaining trapped atoms onto an EMCCD-camera. Numerical image processing finally allows us to determine the number and position of the atoms with nearest neighbour resolution [1].

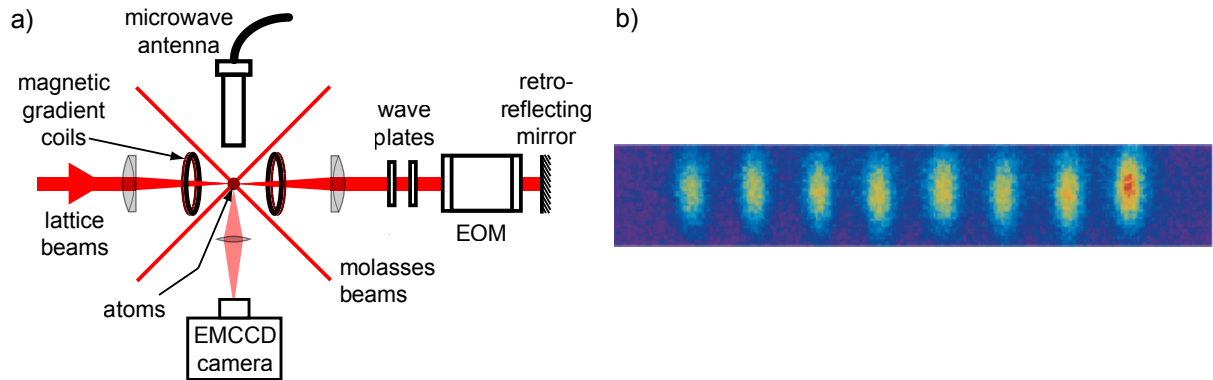


**Figure 1.** (a) Schematic experimental setup. (b) String of eight atoms with a distance of 17 lattice sites ( $\approx 7 \mu\text{m}$ ). The pattern has been prepared by magnetic resonance methods [2]. From the fluorescence images, the position of the atoms can be deduced with single site resolution [1], verifying the targeted inter-atomic distance. The picture is the sum of approximately 50 single fluorescence images.

We use this method to precisely prepare arbitrary patterns of atoms in our 1D lattice by magnetic resonance methods. The lattice is initially filled with many atoms ( $10^2 \dots 10^3$ ). A magnetic field gradient along the lattice axis of  $120 \text{ G/cm}$  spatially detunes the microwave transition between the  $|F = 3, m_F = +3\rangle$  and the  $|F = 4, m_F = +4\rangle$  Zeeman substates by  $30 \text{ kHz}/\mu\text{m}$ . Application of a microwave pulse maps the frequency spectrum onto the spatial population distribution of atoms in  $F = 3$ . After the atoms in  $F = 4$  having been removed from the trap, the spatial occupation distribution reflects the original spectrum of the pulse. For sufficiently narrow Gaussian pulses, single sites of the lattice can be addressed, and thus arbitrary strings of atoms can be designed by a proper choice of pulse frequencies, see Fig.1(b). For details see Ref. [2].

## 2. Atoms in Spin-Dependent Potentials

State-dependent potentials have been proposed originally in order to induce controlled coherent collisions between different trapped atoms [3], and they have been exploited for large scale entanglement in such systems [4]. A state-dependent optical lattice can be visualized as two initially overlapped lattices, where each lattice forms the trap for one of the internal atomic states. If the lattices are shifted with respect to each other, atoms in different internal states can be transported in opposite directions. This entangles the spin degree of freedom with the atomic position, which allows for instance the creation of spatially delocalized quantum states or the control of the atomic motion by microwaves.

### 2.1. Experimental Realisation

It can be shown [3] that at our lattice wavelength of  $\lambda = 866 \text{ nm}$  the two internal states  $|F = 4, m_F = +4\rangle$  and  $|F = 3, m_F = +3\rangle$  couple to a good approximation to only the left- or right-handed circularly polarized components of the light field. Experimentally, the one-dimensional lattice is formed by retro-reflecting a linearly polarized Gaussian laser beam. Its plane of polarization can be rotated by an angle  $\vartheta$  by a combination of an electro-optical modulator (EOM) and passive wave plates, see Fig.1(a). If the lin- $\vartheta$ -lin light field is decomposed into a circular basis, two standing waves emerge which are spatially separated by a distance  $\Delta x = \vartheta \lambda / (2\pi)$ , each trapping atoms in one of the internal states.

The angle  $\vartheta$  is typically set to zero for the MOT-cooling and spin polarisation phases. It can

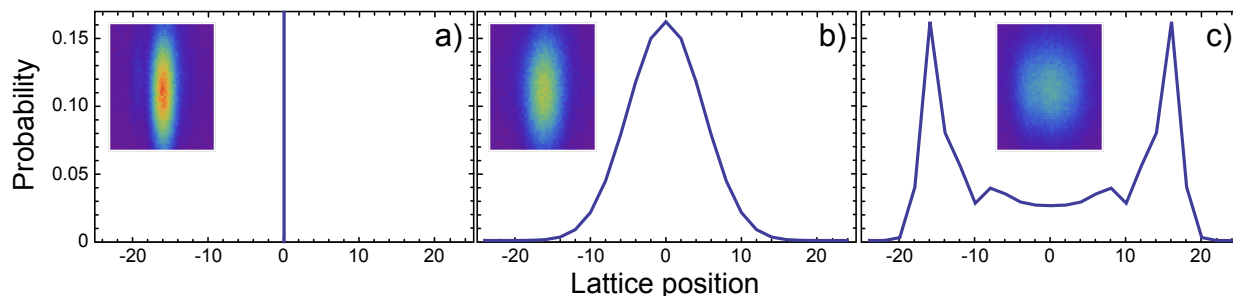


**Figure 2.** Calculated theoretical probability distributions for (a) a localized atom, (b) a random walk, and (c) a quantum walk. The insets show the corresponding atomic wavefunction after experimentally performing a random and a quantum walk with  $N=24$  steps in (b) and (c), respectively. The images are direct superpositions of more than 500 unprocessed individual fluorescence images, thus blurred by our optical resolution of about  $2\ \mu\text{m}$ . The faster spreading due to ballistic expansion of the quantum walk can be clearly seen in comparison to the diffusive spread of the classical random walk.

be continuously rotated in the range between  $[0, \pi]$  by applying a voltage to the EOM. Typical times of voltage ramps are on the order of  $10\ \mu\text{s}$ , implying that such ramps can in principle excite higher vibrational levels [5]. For our usual experiments this is avoided by proper choice of the ramp parameters.

## 2.2. Quantum Walks

The classical random walk is a well known model throughout science, describing a large variety of random processes such as Brownian motion. In a simple case, a particle is walking along a one-dimensional, discrete line. In every time step a coin is tossed, and depending on the random outcome, heads or tails, the particle moves one step to the right or to the left. After  $N$  steps, the probability to find the walker at a certain distance  $d$  away from the initial position follows the well-known binomial distribution, see Fig. 2(b). In particular, the width of this probability distribution scales proportional to  $\sqrt{N}$ .

For a quantum particle, two differences strongly alter this probability distribution: First, a quantum particle can be in a coherent superposition of moving to the left *and* to the right instead of going left *or* right. Thus its wave packet becomes coherently delocalized over several sites of the line. If this procedure is continued, different partial wavepackets of the particle are re-combined at a common site after having gone different paths. Here, matter wave interference occurs, which is the second difference to the classical case. The resulting multi-path matter wave interference strongly alters the probability distribution to find the particle at a certain distance from its initial position, see Fig. 2(c). In particular, the width of this distribution scales linearly with the number of steps  $N$ . This scaling lies at the heart of proposals to exploit this quantum walk phenomenon for quantum search algorithms.

In our experiment, the spin dependent lattice together with coherent microwave radiation to couple the two internal states provides the necessary tool to induce such a quantum walk: An atom is trapped in the lattice and its position is determined by fluorescence imaging. Then, a microwave  $\pi/2$ -pulse creates a coherent superposition of the two internal states. Subsequently, the two states are transported into opposite directions by a shift of the spin dependent lattice. This procedure defines one “step” of the walk, which can be repeated for a given number of steps  $N$ . To detect the distribution of walked distances, fluorescence images of the final positions of many walks are superposed (corrected for the initial positions), see Fig. 2(a-c). If, after every step, the internal state coherence in the system is intentionally destroyed by suitable waiting time

intervals, the classical random walk is recovered. Details can be found in Ref. [6], including the characterization of the quantum walk state by local quantum state tomography, or the coherent reversal of the entire walk by application of a time-inverted sequence. Future applications include single atom interferometry, the generation of atom-atom entanglement by controlled coherent collisions and interacting quantum walks or quantum cellular automata.

### 2.3. Coherent Motional Dynamics

Beyond the ability to create coherent spatially delocalized states, the spin dependent lattice allows tight coherent control of the atomic motion. Traditionally, the quantized motional state of trapped atoms is manipulated by laser light-induced motional sideband transitions. There, the light frequency (photon energy) allows selecting the change of vibrational quanta, and the photon momentum determines the strength of the transition, characterized by the Lamb-Dicke factor. With the microwave fields applied in our experiment, the corresponding photon momentum is roughly five orders of magnitude smaller than in the optical case, and the resulting sideband transition strength is negligible.

The spin dependent lattice, however, offers an alternative way to enable sideband transitions, as different vibrational states in two mutually displaced potentials are no longer orthogonal. Formally this can be cast into the form of an effective Lamb-Dicke parameter, which in our case is not fixed by the choice of photon wavelength, but can be adjusted via the lattice displacement  $\Delta x$ , see Fig. 3(a).

Experimentally, we deduce information about the motional state of the atoms by microwave spectroscopy. While in the case where no lattice shift is applied ( $\vartheta = \Delta x = 0$ ) only the carrier transition can be observed, sidebands emerge if this lattice shift is non-zero, see Fig. 3(b). Based on these sidebands, we have developed a cooling scheme using microwave radiation without the need of phase-locked laser sources, which yields up to 97% ground state population, see Fig. 3(c). Moreover, our method allows us to directly and coherently access all vibrational states in our trap by a single microwave pulse, and to map out the wave function overlap of our trapped atoms with nanometer resolution. For details see Ref. [7]. These techniques may be extended to optical lattices of other wavelengths and to three dimensions, or may be applied to increase the available Hilbert space in quantum information processing by storing an additional qubit in the vibrational states.

## 3. Atoms in a High-Finesse Optical Cavity

Single photons interacting with single atoms form a paradigm of quantum mechanics, where on the one hand quantum effects can be studied in a relatively simple system, and on the other hand novel applications for, e.g., quantum communication can be envisioned.

We realise this paradigm experimentally by inserting single neutral atoms into a high-finesse optical cavity as shown in Fig. 4(a). For details of the experimental setup, see Ref. [8]. In short, the relevant parameters for the coupled system are the coherent atom-field coupling strength  $g$ , the photon decay rate  $\kappa$ , and the atomic decay rate  $\gamma$ , which in our case amount to  $\{g, \kappa, \gamma\}/(2\pi) = \{12, 0.4, 2.6\}$  MHz, where for  $g$  the maximal possible coupling strength for our system has been given.

### 3.1. Quantum Jumps

An intriguing prospect is the application of the cavity to measure the atomic state without destroying it. We approach such a quantum non-demolition measurement by exploiting the normal mode splitting due to the strong coupling of the atom to the cavity field in only one hyperfine state. We tune the probe laser field into resonance with the cavity, and both are slightly blue detuned from the  $F = 4 \rightarrow F' = 5$  transition on the Cs D2-line. While for an empty cavity the resonant probe laser beam would be fully transmitted, the strong coupling

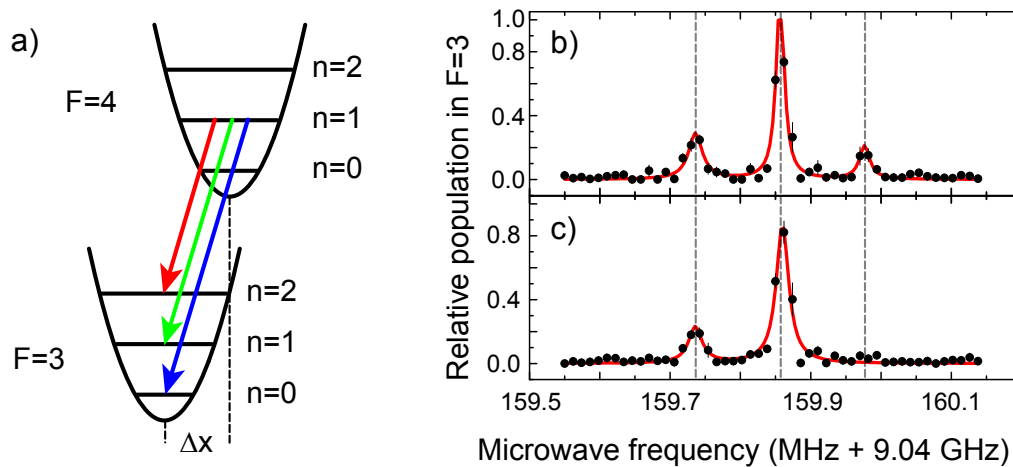


**Figure 3.** (a) If the trapping potentials of the initial and final states are spatially displaced by  $\Delta x$ , the vibrational quantum state can be changed in microwave transitions, even though the photon momentum is negligible. Microwave spectra in a displaced state dependent optical lattice ( $\Delta x = 8$  nm) for (b) molasses cooled atoms, and (c) after microwave cooling on the blue sideband. In the latter case, the absence of the blue sideband indicates an axial ground state population of approximately 98%. In our case, the role of red and blue sidebands are exchanged with respect to the typical case of sideband cooling, because we start from the energetically higher  $F = 4$  state.

of a single atom in the  $F = 4$  hyperfine state leads to the formation of new, frequency-shifted eigenstates according to the well known Jaynes-Cummings model. Hence, the probe laser beam is rather reflected and the transmission level becomes low. If the atom is in the  $F = 3$  hyperfine state, however, it is sufficiently far detuned so that interaction with the cavity field can be neglected and effectively the empty cavity transmission is recovered, i.e., the transmission level of the probe laser beam is high. This method provides a fast means to determine the hyperfine state non-destructively, i.e., neither losing the atom, nor, to good approximation, changing its state by more than a quantum-mechanical projection.

Our quantum non-demolition measurement is not perfect, however, because the atom can be transferred from the  $F = 4$  to the  $F = 3$  state by off-resonant excitation through the cavity field to the  $F' = 4$  state and subsequent decay to  $F = 3$ . By adding a weak additional repumping laser to bring the atom back to  $F = 4$ , the probe laser transmission resembles a random telegraph signal as depicted in Fig. 4, reflecting the quantum jumps of the atomic hyperfine state between the strongly coupled  $F = 4$  and the uncoupled  $F = 3$  state.

An interesting situation arises for two atoms in the resonator. If both atoms have been initially prepared in the same hyperfine state and one atom undergoes a quantum jump, the final state resembles a quantum correlated state, provided no information about the respective state of any atom present can be obtained. It turns out, however, that the two atom telegraph signals do not have sufficient signal-to-noise ratio in order to identify the transmission level where only one atom is in either spin state. Instead of the simple threshold analysis given above, we have analysed the data by a Bayesian analysis using independently obtained information about the system to estimate a conditional probability of the atom to be in a certain spin state at a specific time, given the measured probe laser transmission at this time and the estimated probability at the previous time. This allows us to reconstruct the spin state of the two-atom system with improved fidelity, for details see Ref. [9]. An interesting extension of this method will be a real time analysis by a fast digital signal processor, which opens the possibility for

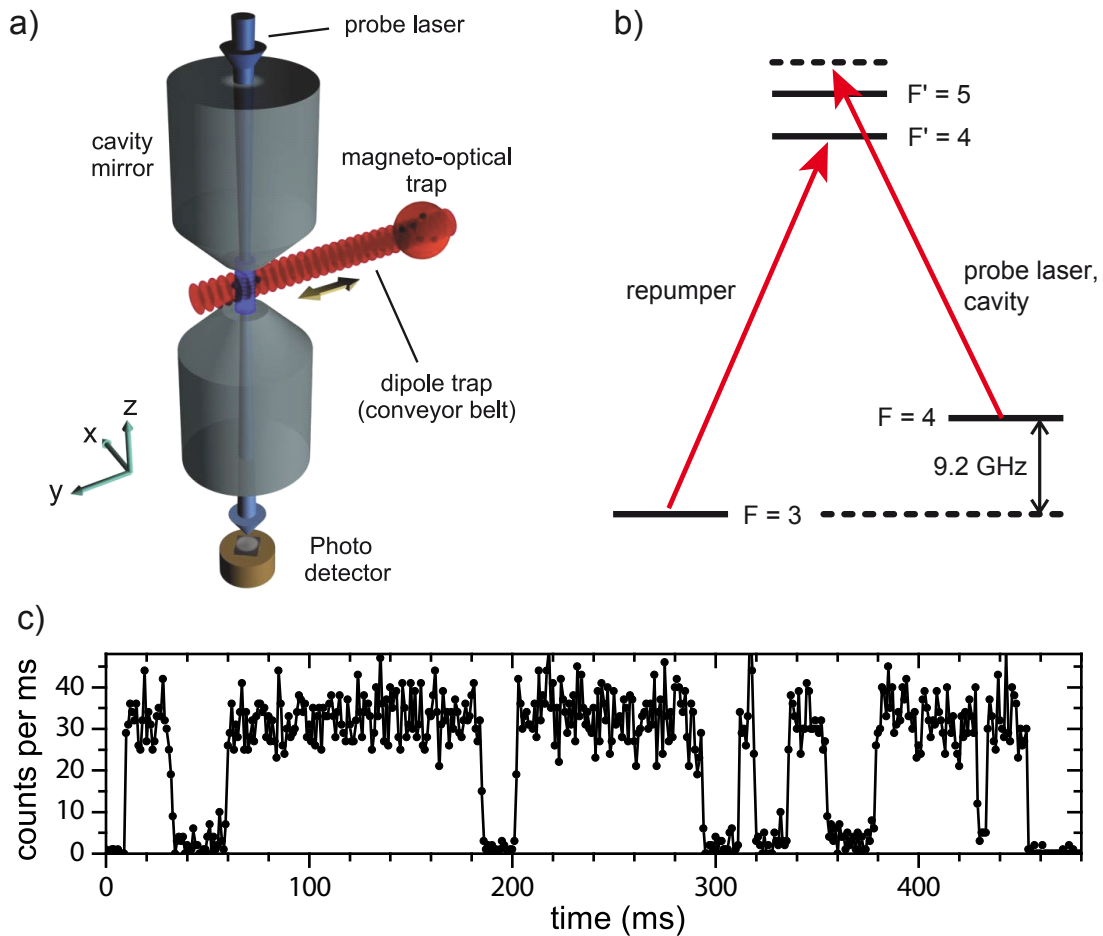


**Figure 4.** (a) Schematics of the experimental setup to couple single and few atoms to a high finesse optical resonator. (b) Relevant level scheme for Cs. The  $F = 4$  ground state is strongly coupled to the resonator, while the  $F = 3$  ground state is far detuned. Excitations to  $F' = 4$  due to the cavity field or an external repumping laser and subsequent decay can change the ground state. (c) Resulting random telegraph signal for the spin state jumping between  $F = 4$  (low transmission level) and  $F = 3$  (high transmission level). For details see Ref. [9].

feedback onto the quantum state of several atoms simultaneously coupled to the cavity.

### 3.2. Controlling the Optical Properties of Single Atoms

Electromagnetically induced transparency (EIT) is a widely known effect in three-level  $\Lambda$ -type systems, where a dense atomic medium becomes transparent for a probe light field when the system is also illuminated by an additional control light field such that the two ground states are coherently coupled [10]. For single atoms the challenge lies in detecting these altered optical properties, as the atom medium has to be initially optically thick to detect a strong change in transmission. Here we have used our high finesse optical resonator to enhance this detection: Due to the strong atom-cavity field coupling, already a single atom can render the system optically thick for the probe laser beam as explained above. If the system is illuminated from the side with a control laser beam phase locked to the probe laser, we observe an increased transmission of the probe laser at the two-photon resonance. A peculiarity of our system is that both laser beams are detuned from the atomic resonance in order to be sensitive to both absorption and

dispersive effects, for details see Ref. [11].

A surprising application of the EIT condition in our system arises from the observation of a strong cooling effect right on the two-photon resonance. We have observed that the storage time of atoms in the dipole trap is almost twenty-fold increased if the two-photon resonance is fulfilled, compared to the case without a control laser beam. In future the Cavity-EIT could be used for storing light in single or few atoms to realize quantum memories, or for performing single-photon-induced optical switching.

### Acknowledgments

Many people have contributed significantly to the experiments outlined in this paper. We gratefully acknowledge enthusiastic work by Andrea Alberti, Noomen Belmechri, Stefan Brakhane, Jai-Min Choi, Martin Eckstein, Leonid Förster, Tobias Kampschulte, Michał Karski, Mkrtych Khudaverdyan, Lingbo Kong, Miguel Martinez Dorantes, Sebastian Reick, René Reimann, Andreas Steffen, and Alexander Thobe. We also thank Poul Jessen and Klaus Mølmer for fruitful collaborations and valuable discussions. We acknowledge financial support from the EU through the IP SCALA and ACQUTE and from the DFG through research unit 635.

### References

- [1] Karski M, Förster L, Choi J M, Alt W, Widera A and Meschede D 2009 *Phys. Rev. Lett.* **102** 053001
- [2] Karski M, Förster L, Choi J, Steffen A, Belmechri N, Alt W, Meschede D and Widera A 2010 *New J. Phys.* **12** 065027
- [3] Jaksch D, Briegel H, Cirac J I, Gardiner C W and Zoller P 1999 *Phys. Rev. Lett.* **82** 1975
- [4] Mandel O, Greiner M, Widera A, Rom T, Hänsch T W and Bloch I 2003 *Nature* **425** 937
- [5] Mandel O, Greiner M, Widera A, Rom T, Hänsch T W and Bloch I 2003 *Phys. Rev. Lett.* **91** 010407
- [6] Karski M, Förster L, Choi J, Steffen A, Alt W, Meschede D and Widera A 2009 *Science* **325** 174
- [7] Förster L, Karski M, Choi J, Steffen A, Alt W, Meschede D, Widera A, Montano E, Lee J, Rakreungdet W and Jessen P S 2009 *Phys. Rev. Lett.* **103** 233001
- [8] Khudaverdyan M, Alt W, Kampschulte T, Reick S, Thobe A, Widera A and Meschede D 2009 *Phys. Rev. Lett.* **103** 123006
- [9] Reick S, Mølmer K, Alt W, Eckstein M, Kampschulte T, Kong L, Reimann R, Thobe A, Widera A and Meschede D 2010 *J. Opt. Soc. Am. B* **27** A152
- [10] Fleischhauer M, Imamoglu A and Marangos J P 2005 *Rev. Mod. Phys.* **77** 633
- [11] Kampschulte T, Alt W, Brakhane S, Eckstein M, Reimann R, Widera A and Meschede D 2010 *Phys. Rev. Lett.* **105** 153603